学術情報リポジトリ

Diffusion of oxygen in amorphous Al_20_3, Ta_20_5, and Nb_20_5

著者	Nakamura R., Toda T., Tsukui S., Tane M., Ishimaru M., Suzuki T., Nakajima H.
journal or publication title	Journal of Applied Physics
volume	116
number	3
year	2014-07-21
権利	(C) 2014 AIP Publishing LLC. This article may be downloaded for personal use only. Any other use requires prior permission of the author and AIP Publishing. The following article may be found at http://scitation.aip.org/content/aip/journal/jap/http://scitation.aip.org/content/aip/journal/jap/101/7/10.1063/1.4889800
URL	http://hdl.handle.net/10466/15023

doi: 10.1063/1.4889800

JOURNAL OF APPLIED PHYSICS **116**, 033504 (2014)

Diffusion of oxygen in amorphous Al_2O_3, Ta_2O_5, and Nb_2O_5

R. Nakamura,[1,a)] T. Toda,[2] S. Tsukui,[1] M. Tane,[2] M. Ishimaru,[3] T. Suzuki,[2] and H. Nakajima[4]
[1]*Department of Materials Science, Graduate School of Engineering, Osaka Prefecture University, Gakuen-cho 1-1, Naka-ku, Sakai 599-8531, Japan*
[2]*The Institute of Scientific and Industrial Research, Osaka University, Mihogaoka 8-1, Ibaraki, Osaka 567-0047, Japan*
[3]*Department of Materials Science and Engineering, Kyushu Institute of Technology, Tobata, Kitakyushu, Fukuoka 804-8550, Japan*
[4]*The Wakasa Wan Energy Research Center, Tsuruga, Fukui 914-0192, Japan*

(Received 3 June 2014; accepted 26 June 2014; published online 15 July 2014)

The self-diffusivity of oxygen in amorphous Al_2O_3 (a-Al_2O_3), a-Ta_2O_5, and a-Nb_2O_5 was investigated along with structural analysis in terms of pair distribution function (PDF). The low activation energy, $\sim$1.2 eV, for diffusion in the oxides suggests a single atomic jump of oxygen ions mediated via vacancy-like defects. However, the pre-exponential factor for a-Ta_2O_5 and a-Nb_2O_5 with lower bond energy was two orders of magnitude larger than that for a-Al_2O_3 with higher bond energy. PDF analyses revealed that the short-range configuration in a-Ta_2O_5 and a-Nb_2O_5 was more broadly distributed than that in a-Al_2O_3. Due to the larger variety of atomic configurations of a-Ta_2O_5 and a-Nb_2O_5, these oxides have a higher activation entropy for diffusion than a-Al_2O_3. The entropy term for diffusion associated with short-range structures was shown to be a dominant factor for diffusion in amorphous oxides. © *2014 AIP Publishing LLC*. [http://dx.doi.org/10.1063/1.4889800]

I. INTRODUCTION

With the recent and rapid advances in nanotechnology and nanoscience, it has become possible to easily and controllably obtain amorphous metal oxides by thin film production processes such as evaporation, sputtering, and atomic layer deposition process, and by chemical routes such as anodic oxidation processes. There is growing interest in amorphous oxides for use as functional materials in a wide range of applications in the field of electrical, optical, chemical, and environmental engineering. For example, amorphous Al_2O_3 (a-Al_2O_3), a-Ta_2O_5, and a-Nb_2O_5 are considered good coating materials for electrical,[1–4] biomedical,[5] and optical devices[6–8] because of their excellent dielectric, corrosion resistance, and reflective properties, respectively. For practical uses, the thermal stability of the layer is an important factor. Knowledge of the diffusional properties in the amorphous oxides is crucial not only to assess their thermal stability and interface stability, but also to be able to tailor the properties of the material. However, knowledge of their diffusion properties is quite limited. To date, only oxygen diffusivity with low activation energy in a-Al_2O_3 has been reported.[9]

Atomic movements in materials are discussed from the perspective of local atomic structures and defect properties. Amorphous oxides are known for the unique structural properties they share. They are much less dense than their counter-part crystalline phases; a-Al_2O_3 (2.8–3.0 g cm^{-3}) and a-Ta_2O_5 (5.0–5.5 g cm^{-3}) are 20% and 30% less dense than γ-Al_2O_3 (3.69 g cm^{-3}) and orthorhombic β-Ta_2O_5 (7.16 g cm^{-3}), respectively,[10,11] indicating that their structures at the atomic-level are highly defective. The structure of a-Al_2O_3 has been actively discussed from the short- and medium-range point-of-view by x-ray photoelectron[12,13] and Auger electron[12] spectroscopy, extended x-ray absorption fine structure technique,[14] transmission electron microscopy,[15,16] nuclear magnetic resonance spectroscopy,[17] and also by a number of theoretical approaches.[18–22] On the other hand, few studies have been reported for a-Ta_2O_5 and a-Nb_2O_5.[23–25]

In this study, the diffusivity of the common element, oxygen, in a-Al_2O_3, a-Ta_2O_5, and a-Nb_2O_5 was investigated. A pair distribution function analysis by transmission electron microscopy was applied since this technique has advantage in describing the overall pictures of local atomic structures for amorphous matters and the change in structure before and after annealing. The diffusion properties of amorphous oxides were clarified by focusing on the short-range atomic structures.

II. EXPERIMENTAL PROCEDURE

A. Diffusion experiment

100 nm-thick films of a-Al_2O_3, a-Nb_2O_5, and a-Ta_2O_5 were prepared; the a-Al_2O_3 films were fabricated by using an electron-beam evaporation technique and the a-Nb_2O_5 and a-Ta_2O_5 films were fabricated by radio-frequency sputtering. A high-purity tablet and target of the crystalline oxide (99.9%–99.99%) were used as the sources for electron-beam evaporation and sputtering, respectively. Films were deposited onto the mirror surface of silicon substrates of $10 \times 5 \times 0.5$ mm^3.

The amorphous oxide on the substrate was subjected to diffusion-annealing for the penetration of ^{18}O. The sample was put into in a quartz-tube electric furnace and pre-annealed under 10^4 Pa of $^{16}O_2$ at a given temperature. Soon

[a)]Author to whom correspondence should be addressed. Electronic mail: nakamura@mtr.osakafu-u.ac.jp. Tel.:+81 72 254 7384. Fax: +81 72 254 9912.

 © 2014 AIP Publishing LLC

[This article is copyrighted as indicated in the article. Reuse of AIP content is subject to the terms at: http://scitation.aip.org/termsconditions. Downloaded to] IP: 157.16.177.79 On: Fri, 18 Jul 2014 13:15:08

after the pre-annealing, $^{16}O_2$ was replaced by $^{18}O_2$ and then diffusion-annealing was performed at the same temperature. To measure the temperature dependence of diffusion coefficients in sufficiently relaxed amorphous oxides, the pre-annealing time, t_p, for $^{16}O_2$ was set at five times longer than the diffusion-annealing time, t, for $^{18}O_2$. It should be noted, however, that t_p was set to be short enough to prevent structural relaxation when measuring the time dependence of the diffusion coefficients at constant temperature. The details of condition setting will be explained later. The penetration profile of ^{18}O was obtained by secondary ion mass spectroscopy (CAMECA SIMS-4100). The film thickness and surface roughness of each sample annealed for diffusion were determined by x-ray reflectometry using a Rigaku SmartLab. The surface roughness was determined to be below 1 nm.

For comparison purposes, the diffusion coefficient in γ-Al_2O_3, which forms during the crystallization of a-Al_2O_3, was also measured. A thin film of γ-Al_2O_3 was obtained by annealing a-Al_2O_3 on a silicon substrate at 1173 K for 4 h in air, which was sufficiently longer than the 5 min set by Nabatame *et al.*[9] The annealing temperature and time were confirmed to be well suited for the crystallization and grain growth of the diffusion sample because the silicon-oxide layer at the Al_2O_3/Si interface became thicker at higher temperature or longer time than the above condition.

B. Structural analysis by transmission electron microscopy

Specimens for cross-sectional TEM observation and for pair distribution analysis were prepared separately. For the cross-sectional observation, the silicon substrate, on which the film was deposited under the same conditions as those mentioned above, was sliced along the thickness direction. Then, it was thinned by a tripod polishing technique, which was followed by argon ion milling. The cross-sectional image and the electron diffraction patterns of the as-deposited and the annealed specimens were observed by a JEOL JEM-3000F TEM at 300 kV.

For a pair distribution function (PDF) analysis, thin films of the amorphous oxides 20–30 nm in thickness were deposited onto cleavage NaCl crystals. The NaCl, on which the thin film was deposited, was put into distilled water, and then the floating thin film was mounted onto a platinum grid. The intensities of the selected-area electron diffraction (SAED) patterns of the plan-view specimens before and after annealing in air were recorded on an imaging plate (Eu^{2+} doped BaFBr) for PDF analysis by TEM at 300 kV. To avoid contamination, electron diffraction intensities were measured at cryogenic temperatures using a cooling holder. The intensities of the as-deposited amorphous oxides were analyzed quantitatively using a Digital Micro-Luminography FDL5000 to obtain the PDF of the amorphous oxides.[26,27]

III. RESULTS AND DISCUSSION

A. Structural analysis

Figure 1 shows cross-sectional TEM images and the corresponding SAED for 100 nm-thick specimens of amorphous Al_2O_3 (a), Ta_2O_5 (b), and Nb_2O_5 (c) before and after annealing in air at 973 K for 4.8 ks, at 800 K for 4.2 ks, and at 650 K for 7.2 ks, respectively. These temperatures are not less than 100 K below their crystallization temperatures, 1073 K for a-Al_2O_3,[28] 923 K for Ta_2O_5,[29] and 823 K for Nb_2O_5.[30] The structures of the specimens were confirmed to remain amorphous after annealing at the conditions. Therefore, the upper limit temperature for diffusion-annealing experiments was considered to be these temperatures.

Figure 2 shows the atomic PDFs for a-Al_2O_3 (a), Ta_2O_5 (b), and Nb_2O_5 (c) obtained by analyzing the SAED patterns of the amorphous regions. As shown in Fig. 2(a), Al-O, O-O, and Al-Al peaks can be seen at around 0.18, 0.28, and 0.32 nm, respectively, which is in good agreement with a number of experimental and simulated PDFs of amorphous Al_2O_3.[16,18–22] The PDF of Ta_2O_5 and Nb_2O_5 is similar with regard to peak position and intensity; peaks for Ta (and Nb)-O, O-O, Ta (Nb)-Ta (Nb) (1), and Ta (Nb)-Ta (Nb) (2) appear at around 0.19, 0.28, 0.34 and 0.37 nm with almost same intensity level (the number in the parenthesis indicates the shorter and longer distance). The common feature is that the

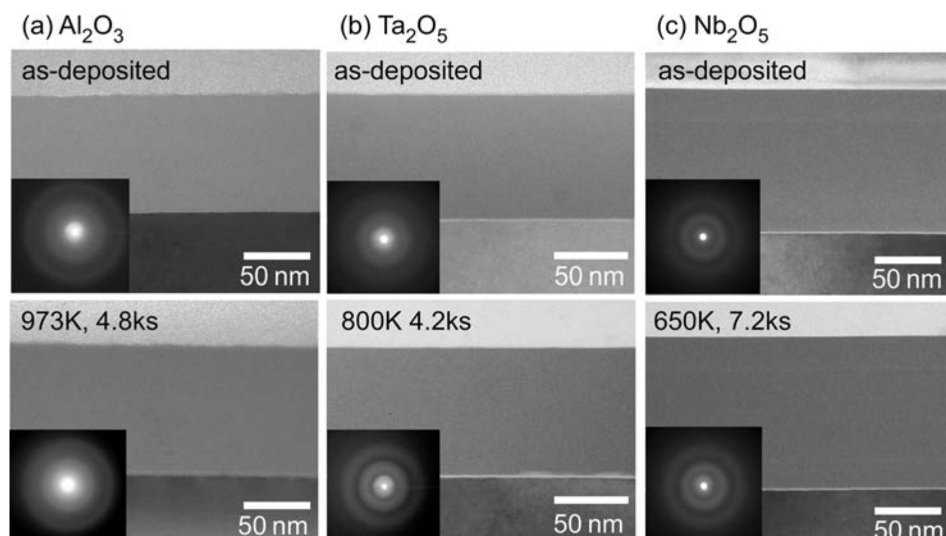

FIG. 1. Cross-sectional TEM images and the corresponding electron diffraction patterns of as-deposited and annealed amorphous oxides: (a) a-Al_2O_3, (b) a-Ta_2O_5, and (c) a-Nb_2O_5.

[This article is copyrighted as indicated in the article. Reuse of AIP content is subject to the terms at: http://scitation.aip.org/termsconditions. Downloaded to] IP: 157.16.177.79 On: Fri, 18 Jul 2014 13:15:08

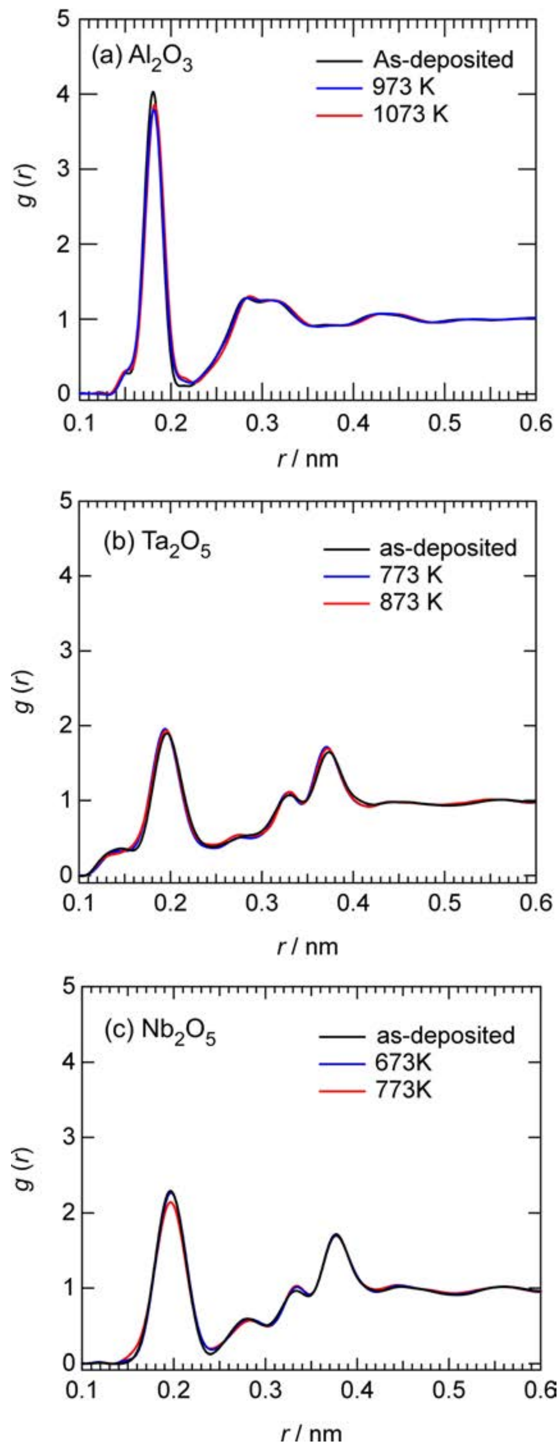

FIG. 2. Pair distribution functions of as-deposited and annealed amorphous oxides: (a) a-Al_2O_3, (b) a-Ta_2O_5, and (c) a-Nb_2O_5. Reprinted with permission for (a) from R. Nakamura, M. Ishimaru, A. Hirata, K. Sato, M. Tane, H. Kimizuka, T. Shudo, T. J. Konno, and H. Nakajima, J. Appl. Phys. **110/6**, 064324-4 (2011). Copyright 2011 AIP Publishing.

PDFs for as-deposited and annealed amorphous oxides are almost consistent with respect to peak intensity and position.

B. Oxygen diffusion

Figures 3(a)–3(d) show an example of the intensity profiles of ^{16}O, ^{18}O, and metal ions of amorphous oxides and γ-Al_2O_3 films after diffusion-annealing in an $^{18}O_2$ atmosphere obtained by SIMS. The intensity of metal ions as well as ^{16}O is almost constant from surface to inside of the film while that of ^{18}O decreases monotonically from the surface and reaches a constant intensity level. The normalized concentration of ^{18}O to total oxygen concentration ($^{16}O + ^{18}O$) was confirmed to reach the natural abundance of ^{18}O, around 0.2%, which corresponds to the background concentration C_{bg}. The condition used for the exchange annealing corresponds to a semi-infinite medium with a surface concentration, C_s, constant. The approximate solution for Fick's second law is expressed as

$$\mathrm{erfc}^{-1}\left\{\frac{C(x)-C_{bg}}{C_s-C_{bg}}\right\}=\frac{x}{2\sqrt{Dt}} \tag{1}$$

under the initial condition of $C(x) = C_{bg}$ for $t = 0$ and $x > 0$, and $C(x) = C_s$ for $x = 0$, where x and t are diffusion distance and time, respectively. From the slope for the plots of inverse error function against x, as shown in Fig. 4, the diffusion coefficient of oxygen was determined by using Eq. (1).

The effect of structural relaxation on the diffusion properties in amorphous metals and metallic glasses has been investigated; diffusion coefficients have a tendency to decrease as a function of annealing time and then reach a constant value at a steady, relaxed amorphous state.[31] In such a case, a diffusion coefficient obtained by the solution of Fick's second law is regarded as a time-averaged value, $\bar{D}(t) = \frac{1}{t}\int_0^t D(t)\mathrm{d}t$, for the time-dependent diffusion coefficients $D(t)$, as illustrated in Fig. 5(a). An attempt to estimate time-dependent diffusion coefficients has been made for amorphous metals and metallic glasses[31] by using the equation below

$$D(t) = \bar{D}(t) + t\frac{\mathrm{d}\bar{D}(t)}{\mathrm{d}t}. \tag{2}$$

To apply Eq. (2), many experimental data are required to solve the equation. In the present study, we developed an alternative method to obtain time-dependent diffusion coefficients which can be applied when the number of experimental data is limited. When a diffusion coefficient is determined by using Eq. (1), a time-averaged diffusion coefficient, $\bar{D}_n = \frac{1}{n\Delta t}\int_0^{n\Delta t} D(t)\mathrm{d}t$, is obtained for the diffusion-annealing time $n\Delta t$, as shown in Fig. 5(a). The obtained $\bar{D}_n$ clearly deviates from the intrinsic diffusion coefficient $D(t)$, as shown in Fig. 5(a). However, by measuring the time-averaged diffusion coefficients $\bar{D}_n$ for different annealing times, time-segmented diffusion coefficients D_n for time-segments Δt ($=n\Delta t - (n-1)\Delta t$), shown in Fig. 5(b), can be evaluated. It should be noted that the averaging times are different between the coefficients $\bar{D}_n$ and D_n, and the coefficient D_n must be closer to the intrinsic diffusion coefficient $D(t)$, because the averaging time is shorter. The concept of the evaluation of D_n is based on the time-segmentation of atomic jumps, as explained in the Appendix in detail. Since the number of atomic jumps during total diffusion time $n\Delta t$ is equal to the sum of time-segmented atomic jumps during Δt, $\bar{D}_n$ can be expressed by D_n as follows:

[This article is copyrighted as indicated in the article. Reuse of AIP content is subject to the terms at: http://scitation.aip.org/termsconditions. Downloaded to] IP: 157.16.177.79 On: Fri, 18 Jul 2014 13:15:08

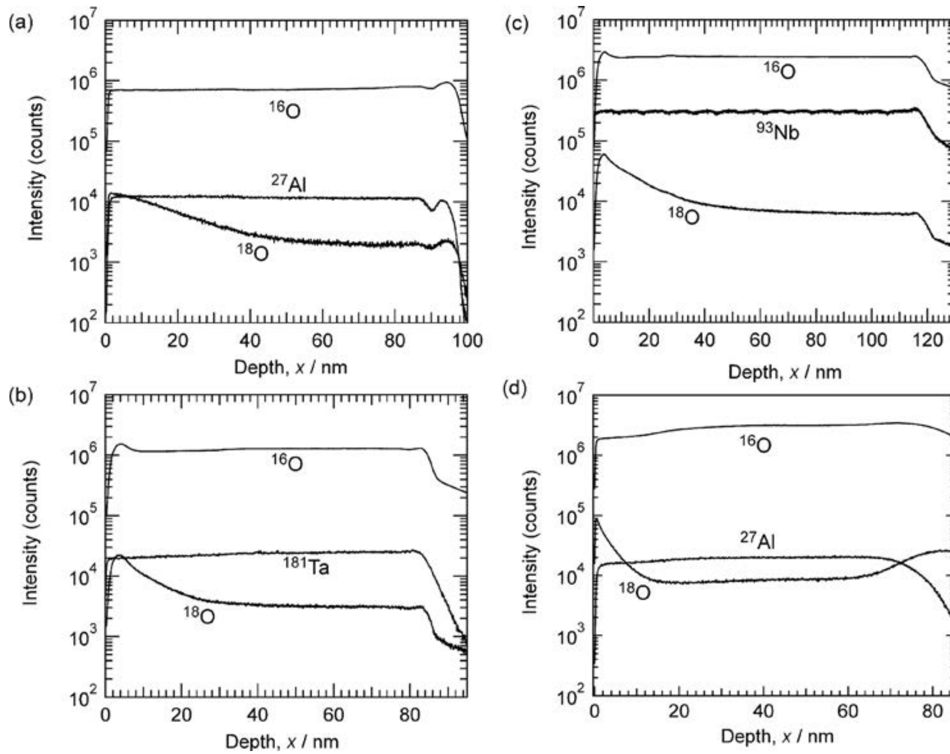

FIG. 3. An example of intensity-depth profile of ^{16}O, ^{18}O, and metal ions in amorphous oxides (a) a-Al_2O_3 at 900 K for 19.8 ks, (b) a-Ta_2O_5 at 675 K for 9.9 ks, and (c) a-Nb_2O_5 at 625 K for 1.8 ks, and in (d) γ-Al_2O_3 at 1023 K for 331.2 ks.

$$n\bar{D}_n\Delta t = \sum_{i=1}^{n} D_i \Delta t\{i-(i-1)\}$$
$$= D_1\Delta t + D_2\Delta t + \cdots + D_n\Delta t, \quad (3)$$

where $D_1 = \bar{D}_1$. When we measure the averaged diffusion coefficients $\bar{D}_1(=D_1)$, $\bar{D}_2$, and $\bar{D}_3$ for Δt, $2\Delta t$, and $3\Delta t$, respectively, D_2 is calculated from $\bar{D}_2$ and D_1, and then D_3 is calculated from $\bar{D}_3$, D_2, and D_1 using Eq. (3), sequentially. The value of D_n can be obtained more accurately by setting the time-segment Δt smaller. In our experiments, t was set to be $1.8 \sim 7.2$ ks for $n = 1 \sim 4$ and $\Delta t = 1.8$ ks. $\bar{D}_n$ and D_n of oxygen obtained at 873 and 973 K in a-Al_2O_3 are summarized in Table I and plotted against $t/2$ and $t-\Delta t/2$, respectively, in Fig. 6. The effect of structural relaxation on the diffusion coefficients is clearly seen in the time-dependence of D_n rather than time-averaged $\bar{D}_n$. The degree of relaxation seems to be about one order, which is similar to that for metallic glasses.[31]

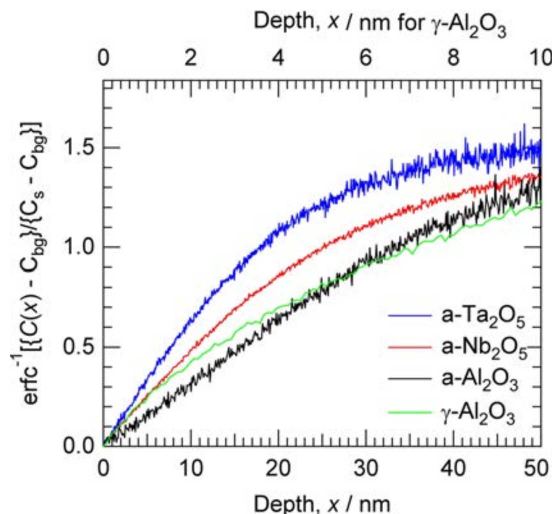

FIG. 4. Concentration profiles of oxygen converted from Fig. 3 through the Eq. (1). The lower scale is for a-Al_2O_3, a-Nb_2O_5, and a-Ta_2O_5, while the upper scale is for γ-Al_2O_3.

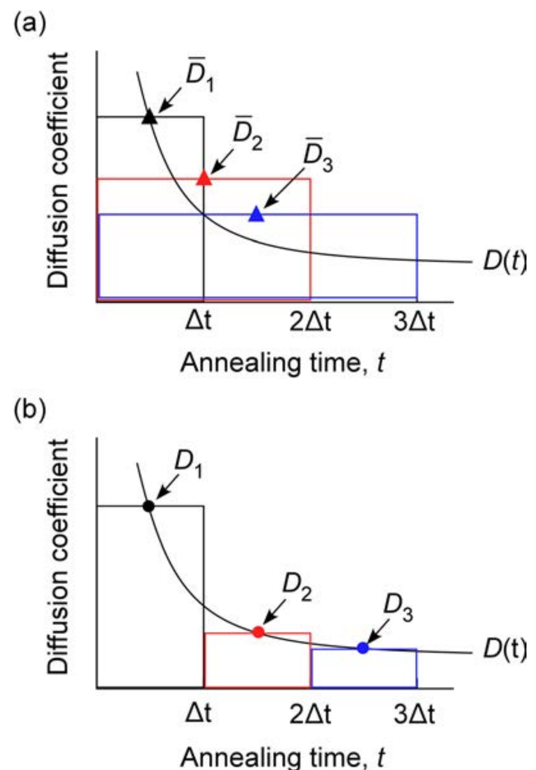

FIG. 5. Schematic illustrations of time-dependent diffusion coefficient. (a) Time-averaged values $\bar{D}_n$ obtained through Eq. (1). (b) An idea to estimate D_n by using $\bar{D}_n$ during a uniform time-segment.

[This article is copyrighted as indicated in the article. Reuse of AIP content is subject to the terms at: http://scitation.aip.org/termsconditions. Downloaded to] IP: 157.16.177.79 On: Fri, 18 Jul 2014 13:15:08

TABLE I. Diffusion coefficients in a-Al_2O_3 at 873 and 973 K evaluated as functions of annealing time. Pre-annealing time was set as 1.8 ks for all the measurements.

T	n	t	$\bar{D}_n$/m^{2}s^{-1}	$t-\Delta t/2$	D_n/m^{2}s^{-1}
873	1	1.8	1.5×10^{-20}	0.9	1.5×10^{-20}
	2	3.6	1.0×10^{-20}	2.7	5.2×10^{-21}
	3	5.4	8.2×10^{-21}	4.5	4.5×10^{-21}
	4	7.2	7.2×10^{-21}	6.3	4.2×10^{-21}
973	1	1.8	1.4×10^{-19}	0.9	1.4×10^{-19}
	2	3.6	8.9×10^{-20}	2.7	4.0×10^{-20}
	3	5.4	6.9×10^{-20}	4.5	2.9×10^{-20}

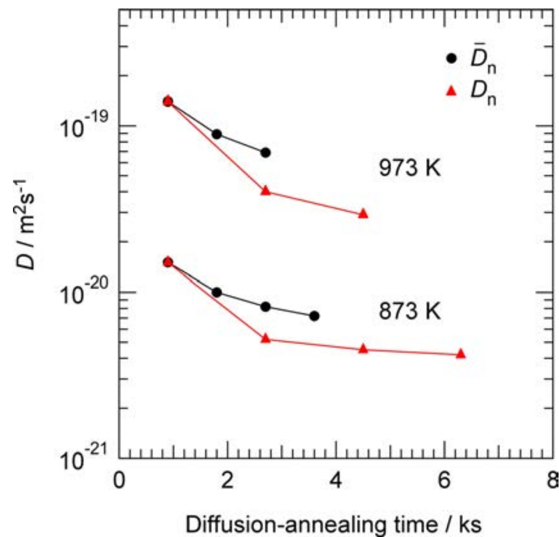

FIG. 6. Time-averaged diffusion coefficients $\bar{D}_n$ and time-dependent diffusion coefficients D_n at 873 and 973 K in a-Al_2O_3 plotted against diffusion-annealing time.

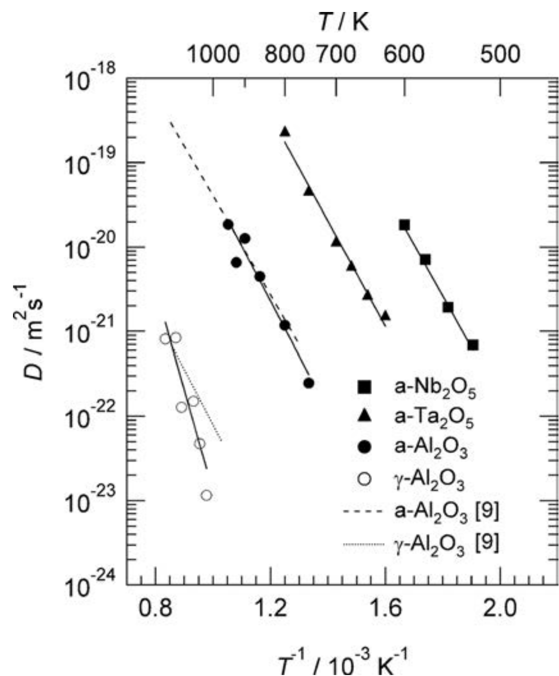

FIG. 7. Temperature dependence of oxygen diffusion coefficients in amorphous oxides and γ-Al_2O_3.

TABLE II. Diffusion coefficients in relaxed state of amorphous Al_2O_3, Ta_2O_5, Nb_2O_5, and γ-Al_2O_3.

Oxides	T/K	^{16}O annealing time, t_p/ks	^{18}O annealing time, t/ks	D/m^{2}s^{-1}
a-Al_2O_3	750	589.2	144	2.5×10^{-22}
	800	259	87.6	1.2×10^{-21}
	860	216	73.2	4.5×10^{-21}
	900	109.8	19.8	1.3×10^{-20}
	925	72	14.4	6.6×10^{-21}
	950	61.2	19.8	1.9×10^{-20}
γ-Al_2O_3	1023	439.2	331.2	1.2×10^{-23}
	1073	187.2	172.8	1.5×10^{-22}
	1123	123.3	87.3	1.3×10^{-22}
	1148	84	64.5	8.4×10^{-22}
	1198	10.8	7.2	8.1×10^{-22}
a-Ta_2O_5	625	219.6	73.2	1.5×10^{-21}
	650	54	16.2	2.6×10^{-21}
	675	35.1	9.9	5.7×10^{-21}
	700	61.2	7.56	1.1×10^{-20}
	750	45	1.8	4.5×10^{-20}
	800	3.6	0.6	2.3×10^{-19}
a-Nb_2O_5	500	248.2	98.1	4.3×10^{-22}
	525	64.8	18	6.9×10^{-22}
	550	21.6	7.2	1.9×10^{-21}
	575	10.2	1.8	7.1×10^{-21}
	600	5.4	1.56	1.8×10^{-20}
	625	11.7	1.8	5.3×10^{-20}
	650	6.0	1.2	6.7×10^{-20}

The temperature dependence of D in sufficiently-relaxed amorphous oxides and in γ-Al_2O_3 is shown in Fig. 7. The diffusion coefficients for each annealing condition, and the activation energy Q and pre-exponential factor D_0 for oxygen diffusion are summarized in Tables II and III, respectively. The value of D in a-Al_2O_3 is in good agreement with that obtained by Nabatame *et al.* (broken line).[9] Q of a-Al_2O_3, 1.3 eV, obtained in the present work agrees well with that reported by Nabatame *et al.*, 1.2 eV. D in γ-Al_2O_3 in the present work is about three orders of magnitude smaller than D in a-Al_2O_3 in the same temperature range. The large discrepancy in D in γ-Al_2O_3 between the present work and the literature data can be seen particularly at low temperature region. As a result, Q of the present work, 2.4 eV, is twice as large as that of Nabatame *et al.*, 1.3 eV. This indicates that a crystalline phase with lower diffusivity has a higher activation energy than its amorphous phase with higher diffusivity. As mentioned in Sec. II A, we set the annealing time for the preparation of γ-Al_2O_3 from a-Al_2O_3 at a much longer time than that used by Nabatame *et al.* for the purpose of grain

TABLE III. Activation energy Q and frequency factor D_0 for oxygen diffusion in the amorphous oxides and γ-Al_2O_3.

Oxides	Q / eV	D_0 / m^{2}s^{-1}
a-Al_2O_3	1.3 ± 0.2	$8.6^{+58}_{-7.5}\times10^{-14}$
γ-Al_2O_3	2.4 ± 0.3	$1.7^{+75}_{-1.6}\times10^{-11}$
a-Ta_2O_5	1.2 ± 0.1	$8.6^{+2.2}_{-0.73}\times10^{-11}$
a-Nb_2O_5	1.0 ± 0.1	$9.4^{+27}_{-7.0}\times10^{-12}$

[This article is copyrighted as indicated in the article. Reuse of AIP content is subject to the terms at: http://scitation.aip.org/termsconditions. Downloaded to] IP: 157.16.177.79 On: Fri, 18 Jul 2014 13:15:08

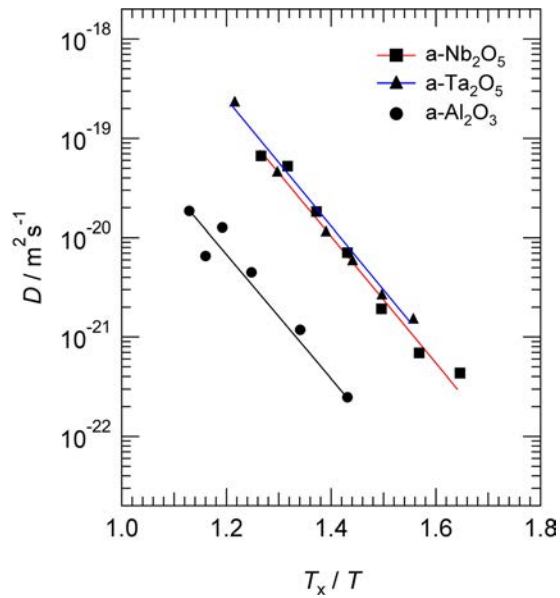

FIG. 8. Diffusion coefficients of oxygen plotted against temperature normalized by crystallization temperature T_x in amorphous oxides.

growth and increased crystallinity. The discrepancy seems to be attributed to the difference in annealing condition for crystallization and grain growth to obtain γ-Al_2O_3 from a-Al_2O_3.

The diffusion coefficient of oxygen in the amorphous oxides is in the order of $Nb_2O_5 > Ta_2O_5 > Al_2O_3$, as shown in Fig. 7. Although Q of these oxides lies in the range of 1.0–1.3 eV, D_0 of Nb_2O_5 and Ta_2O_5 is about two orders of magnitude larger than that of a-Al_2O_3. For metallic glasses, a corporative motion involving a cluster of neighboring atoms is operative with higher activation energy around 4 eV while a single jump motion occurs independently with a small activation energy around $1 \sim 2$ eV.[31,32] The small activation energies for diffusion in amorphous oxides can be interpreted as a single jump motion. As mentioned above, the crystallization temperature T_x of a-Al_2O_3, a-Ta_2O_5, and a-Nb_2O_5 has been reported to be 1073 K, 973 K, and 823 K, respectively. Diffusivity among the oxides is clearly categorized in Fig. 8, where D is plotted against normalized temperature T_x/T; D in a-Ta_2O_5 is almost consistent with that in a-Nb_2O_5, while that in a-Al_2O_3 is far smaller than the others. The good consistence in diffusivity between a-Ta_2O_5 and a-Nb_2O_5 must reflect their structural similarity, as shown in the pair distribution functions of Fig. 2.

The activation energy Q and the pre-exponential factor D_0 for self-diffusion in solids, particularly, in metals, are empirically correlated to bulk properties such as melting point, cohesive energy, and elastic constant[33,34] since atomic diffusion is governed by the nature and strength of the cohesion in the matrix. Figure 9(a) shows the relationship between the diffusion parameters (Q and D_0) for oxygen diffusion in metastable a-Al_2O_3 and γ-Al_2O_3, and stable α-Al_2O_3 (Ref. 35) and their enthalpy. The value of α-Al_2O_3 is shown as a range of some reliable data. Enthalpy in this case ($-\Delta E$) is a difference with a-Al_2O_3 as a standard state.[22] Q and D_0 increase with increasing enthalpy difference, namely, phase stability. The extreme increase from

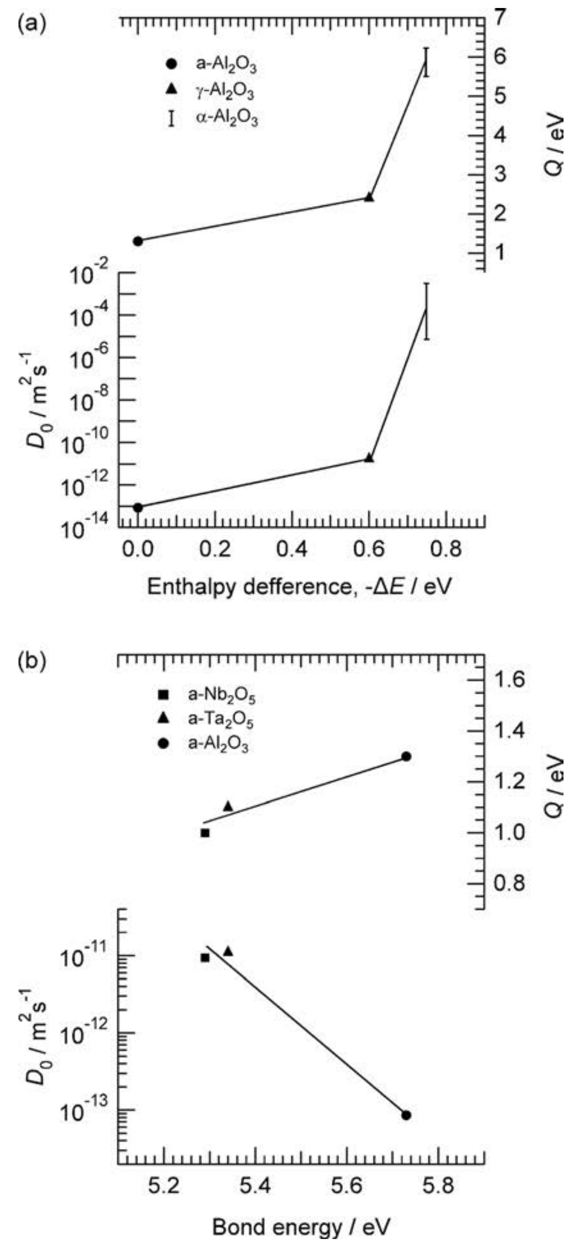

FIG. 9. Relationship between diffusion parameters (activation energy and pre-exponential factor) and bulk properties (enthalpy difference and bond energy) among (a) Al_2O_3 phases and (b) amorphous oxides.

γ-Al_2O_3 to α-Al_2O_3 is a unique trend at the transition from the metastable phase to stable phase. However, the general trend conforms to the empirical correlation; Q and D_0 among Al_2O_3 phases increase along with stabilization of phase and increase in cohesion.

For the amorphous oxides, Q and D_0 are plotted against the binding energy between metal and oxygen ions,[36] as shown in Fig. 9(b). As mentioned above, Q of the amorphous oxides lies in $1.0 \sim 1.3$ eV and shows a weak increase against binding energy. Interestingly, D_0 of these amorphous oxides shows a negative correlation with binding energy; it decreases with increasing binding energy. Pre-exponential factor for diffusion is expressed as

$$D_0 = gfd^2 v_0 \exp\left(\frac{\Delta S}{k_B}\right), \quad (4)$$

[This article is copyrighted as indicated in the article. Reuse of AIP content is subject to the terms at: http://scitation.aip.org/termsconditions. Downloaded to] IP: 157.16.177.79 On: Fri, 18 Jul 2014 13:15:08

where g is a geometric factor, d the effective jump distance, ν_0 the effective jump-attempt frequency, f the correlation factor, and ΔS the activation entropy for diffusion. In general, D_0 represents elastic property behind the jump frequency. In the case of amorphous oxides, the jump distance most likely corresponds to oxygen-oxygen bond length. As can be seen in the PDF of Fig. 2, the bond-length of oxygen ions, d, is around 0.28 nm in a-Al_2O_3, a-Ta_2O_5, and a-Nb_2O_5. Although the value of the other factors, g and f, depends on the short-range configuration, the difference among these oxides is probably not so large. Since the large difference in D_0 between a-Al_2O_3, and a-Ta_2O_5 and a-Nb_2O_5 cannot be understood by a difference in the term, $gfd^2\nu_0$, the main effect must come from the entropy term of Eq. (4). In the case of amorphous matrices, D_0 is linked not to a formation entropy of defects, but to a migration entropy since diffusion is believed to occur without the formation of point defects as in crystals. It is known that the value of ΔS for amorphous alloys lies in the range $19k_B$–$56k_B$, which are much higher than $2.5k_B$–$7.5k_B$ for crystalline cases.[31] The value of ΔS for amorphous alloys would also include the contribution from increased configurational entropy,[31] suggesting that the variety of atomic configuration is a determining factor for ΔS and therefore D_0 as well. According to extensive studies on the atomic configuration of amorphous Al_2O_3, it is commonly accepted that amorphous Al_2O_3 is composed of a majority of AlO_4 and AlO_5 basic units, and a minority of AlO_6 units. On the other hand, amorphous Ta_2O_5 has a wider variety of basic units TaO_x ($x = 3$–7).[23] In fact, the first peak for Ta-O bonds around 0.2 nm is more broadly distributed than that for Al-O bonds, suggesting also a wide variety of configuration around oxygen ions. It must be also the case for a-Nb_2O_5 because of the similarity in PDF (Fig. 2). It seems that the higher values of D_0 in a-Ta_2O_5 and a-Nb_2O_5 than a-Al_2O_3 are derived from a wider variety of short-range configuration in a-Ta_2O_5 and a-Nb_2O_5.

IV. CONCLUSION

Activation energy for oxygen diffusion in amorphous Al_2O_3, Ta_2O_5, and Nb_2O_5 oxides lies in the comparable values between 1.0 and 1.3 eV. On the other hand, the large difference in frequency factor D_0 for diffusion was found; the value of D_0 around $1.0 \times 10^{-11}\,m^2\,s^{-1}$ for a-Ta_2O_5 and a-Nb_2O_5 with a lower bond energy is two orders of magnitude larger than $8.6 \times 10^{-14}\,m^2\,s^{-1}$ for a-Al_2O_3 with a higher bond energy. It should be noted that the magnitude of the pre-exponential factor shows a negative correlation against the bond energy among these amorphous oxides. The determining factor for the large difference in D_0 in amorphous oxides can be derived from the difference in configuration entropy. The variety of short-range configuration such as bond length and coordination number is necessary for diffusion properties in amorphous oxides to be determined.

ACKNOWLEDGMENTS

This work was supported by Grant-in-Aid for Young Scientists (B) (No. 24760574). The analyses by SIMS and TEM were performed under the Cooperative Research Program of "Network Joint Research Center for Materials and Devices".

APPENDIX: TIME-SEGMENTATION OF ATOMIC JUMP

A diffusion coefficient D and the number of atomic jump N are related to jump frequency Γ and jump distance d,

$$D = \Gamma d^2, \tag{A1}$$

$$\Gamma = \frac{N}{t}. \tag{A2}$$

Thus, D multiplied by the annealing time t is expressed by the number of atomic jump N and a jump distance d,

$$Dt = Nd^2. \tag{A3}$$

For the time-averaged diffusion coefficient $\bar{D}_n$, the following equation holds;

$$\bar{D}_n \cdot n\Delta t = Nd^2, \tag{A4}$$

where it is assumed that d is constant during $n\Delta t$. On the other hand, for the time-segmented diffusion coefficient D_n, Eq. (A5) is satisfied as

$$D_1\Delta t + D_2\Delta t + \cdots + D_n\Delta t = (N_1 + N_2 + \cdots + N_n)d^2. \tag{A5}$$

Since $N_1 + N_2 + \cdots + N_n = N$ is satisfied, we obtain

$$\bar{D}_n \cdot n\Delta t = D_1\Delta t + D_2\Delta t + \cdots + D_n\Delta t. \tag{A6}$$

[1] Y. N. Novikov, V. A. Gritsenko, and K. A. Nasyrov, Appl. Phys. Lett. **94**, 222904 (2009).
[2] H. Shinriki, T. Kisu, S. I. Kimura, Y. Nishioka, Y. Kawamoto, and K. Mukai, IEEE Trans. Electron Devices **37**, 1939 (1990).
[3] M. Tauseef Tanvir, Y. Aoki, and H. Habazaki, Appl. Surf. Sci. **255**, 8383 (2009).
[4] K. Kukli, M. Ritala, and M. Leskela, J. Electrochem. Soc. **148**, F35 (2001).
[5] Y. L. Zhou, M. Niinomi, T. Akahori, H. Fukui, and H. Toda, Mater. Sci. Eng. A **398**, 28 (2005).
[6] R. F. Cava, W. F. Peck, and J. J. Krajewski, Nature **377**, 215 (1995).
[7] J. M. Ngaruiya, O. Kappertz, S. H. Mohamed, and M. Wuttig, Appl. Phys. Lett. **85**, 748 (2004).
[8] M. Vinnichenko, A. Rogozin, D. Grambole, F. Munnik, A. Kolitsch, W. Möller, O. Stenzel, S. Wilbrandt, A. Chuvilin, and U. Kaiser, Appl. Phys. Lett. **95**, 081904 (2009).
[9] T. Nabatame, T. Yasuda, M. Nishizawa, M. Ikeda, T. Horikawa, and A. Toriumi, Jpn. J. Appl. Phys. **42**, 7205 (2003).
[10] I. Levin and D. Brandon, J. Am. Ceram. Soc. **81**, 1995 (1998).
[11] D. Lüzenkirchen-Hecht and R. Frahm, Physica B: Condensed Matter **283**, 108 (2000).
[12] Y. Kameshima, A. Yasumori, and K. Okada, Hyomen Kagaku **21**, 481 (2000).
[13] P. C. Snijders, L. P. H. Jeurgens, and W. G. Sloof, Surf. Sci. **589**, 98 (2005).
[14] S. M. El-mashri, R. G. Jones, and A. J. Forty, Philos. Mag. A **48**, 665 (1983).
[15] D. Bouchet and C. Colliex, Ultramicroscopy **96**, 139 (2003).
[16] R. Nakamura, M. Ishimaru, H. Yasuda, and H. Nakajima, J. Appl. Phys. **113**, 064312 (2013).
[17] S. K. Lee, S. B. Lee, S. Y. Park, Y. S. Yi, and C. W. Ahn, Phys. Rev. Lett. **103**, 095501 (2009).

[This article is copyrighted as indicated in the article. Reuse of AIP content is subject to the terms at: http://scitation.aip.org/termsconditions. Downloaded to] IP: 157.16.177.79 On: Fri, 18 Jul 2014 13:15:08

[18]P. Lamparter and R. Kniep, Phys. B: Condensed Matter. **234–236**, 405 (1997).
[19]G. Gutierrez and B. Johansson, Phys. Rev. B. **65**, 104202 (2002).
[20]P. Vashishta, R. K. Kalia, A. Nakano, and J. P. Rino, J. Appl. Phys. **103**, 083504 (2008).
[21]A. R. Ferreira, E. Kücükbenli, A. A. Leitao, and S. de Gironcoli, Phys. Rev. B **84**, 235119 (2011).
[22]M. Tane, S. Nakano, R. Nakamura, H. Ogi, M. Ishimaru, H. Kimizuka, and H. Nakajima, Acta Mater. **59**, 4631 (2011).
[23]R. Bassiri, K. B. Borisenko, D. J. H. Cockayne, J. Hough, I. MacLaren, and S. Rowan, Appl. Phys. Lett. **98**, 031904 (2011).
[24]N. Kim and J. F. Stebbins, Chem. Mater. **23**, 3460 (2011).
[25]R. J. Bondi, M. P. Desjarlais, A. P. Thompson, G. L. Brennecka, and M. J. Marinella, J. Appl. Phys. **114**, 203701 (2013).
[26]Y. Hirotsu, M. Ishimaru, T. Ohkubo, T. Hanada, and M. Sugiyama, J. Electron Microsc. **50**, 435 (2001).
[27]M. Ishimaru, Nucl. Instrum. Methods Phys. Res. B **250**, 309 (2006).
[28]R. Nakamura, T. Shudo, A. Hirata, M. Ishimaru, and H. Nakajima, Scr. Mater. **64**, 197 (2011).
[29]R. Nakamura, K. Tanaka, M. Ishimaru, K. Sato, T. J. Konno, and H. Nakajima, Scr. Mater. **66**, 182 (2012).
[30]R. Nakamura, M. Ishimaru, K. Sato, K. Tanaka, H. Nakajima, and T. J. Konno, J. Appl. Phys. **114**, 124308 (2013).
[31]F. Faupel, W. Frank, M.-P. Macht, H. Mehrer, V. Naundorf, K. Rätzke, H. R. Schober, S. K. Sharma, and H. Teichler, Rev. Modern Phys. **75**, 237 (2003).
[32]U. Geyer, S. Schneider, W. L. Johnson, Y. Qiu, T. A. Tombrello, and M. P. Macht, Phys. Rev. Lett. **75**, 2364 (1995).
[33]C. Wert and C. Zener, Phys. Rev. **76**, 1169 (1949).
[34]G. P. Tiwari, R. S. Mehrota, and Y. Iijima, *Diffusion Processes in Advanced Technological Materials*, edited by D. Gupta (William Andrew, Inc., 2005), p. 69.
[35]A. H. Heuer, J. Eur. Ceram. Soc. **28**, 1495 (2008).
[36]A. K. Vijh, J. Electrochem. Soc. **116**, 972 (1969).

[This article is copyrighted as indicated in the article. Reuse of AIP content is subject to the terms at: http://scitation.aip.org/termsconditions. Downloaded to] IP: 157.16.177.79 On: Fri, 18 Jul 2014 13:15:08